haematologica

Journal of The Ferrata Storti Foundation

Immunodeficiency, autoimmune thrombocytopenia and enterocolitis caused by autosomal recessive deficiency of PIK3CD-encoded phosphoinositide 3-kinase

by David J Swan, Dominik Aschenbrenner, Christopher A Lamb, Krishnendu Chakraborty, Jonathan Clark, Sumeet Pandey, Karin R Engelhardt, Rui Chen, Athena Cavounidis, Yuchun Ding, Natalio Krasnogor, Christopher D Carey, Meghan Acres, Stephanie Needham, Andrew J Cant, Peter D Arkwright, Anita Chandra, Klaus Okkenhaug, Holm H Uhlig, and Sophie Hambleton

Haematologica 2019 [Epub ahead of print]

Citation: David J Swan, Dominik Aschenbrenner, Christopher A Lamb, Krishnendu Chakraborty, Jonathan Clark, Sumeet Pandey, Karin R Engelhardt, Rui Chen, Athena Cavounidis, Yuchun Ding, Natalio Krasnogor, Christopher D Carey, Meghan Acres, Stephanie Needham, Andrew J Cant, Peter D Arkwright, Anita Chandra, Klaus Okkenhaug, Holm H Uhlig, and Sophie Hambleton. Immunodeficiency, autoimmune thrombocytopenia and enterocolitis caused by autosomal recessive deficiency of PIK3CD-encoded phosphoinositide 3-kinase.
Haematologica. 2019; 104:xxx
doi:10.3324/haematol.2018.208397

Immunodeficiency, autoimmune thrombocytopenia and enterocolitis caused by autosomal recessive deficiency of *PIK3CD*-encoded phosphoinositide 3-kinase δ

David J. Swan[1]*, Dominik Aschenbrenner[2]*, Christopher A. Lamb[1,3]*, Krishnendu Chakraborty[4], Jonathan Clark[4], Sumeet Pandey[2], Karin R. Engelhardt[1], Rui Chen[1], Athena Cavounidis[2], Yuchun Ding[5], Natalio Krasnogor[5],Christopher D. Carey[3], Meghan Acres[1,3], Stephanie Needham[3], Andrew J. Cant[3], Peter D. Arkwright[6], Anita Chandra[4,7], Klaus Okkenhaug[4,8], Holm H. Uhlig[2,9,10]**, Sophie Hambleton[1,3]**

* and ** joint authorship

1 Institute of Cellular Medicine, Newcastle University, Newcastle upon Tyne, UK.
2 Translational Gastroenterology Unit, John Radcliffe Hospital, University of Oxford, Oxford, UK.
3 Newcastle upon Tyne Hospitals NHS Foundation Trust, Newcastle upon Tyne, UK.
4 Babraham Institute, Cambridge, UK
5 School of Computing Science, Newcastle University, Newcastle upon Tyne, UK
6 University of Manchester & Department of Paediatric Allergy & Immunology, Royal Manchester Children's Hospital, Manchester, UK
7 Department of Medicine, University of Cambridge, Cambridge, UK.
8 Division of Immunology, Department of Pathology, University of Cambridge, Cambridge, UK.
9 Department of Paediatrics, University of Oxford, Oxford, UK.
10 Oxford NIHR Biomedical Research Centre, Oxford, UK

Corresponding authors:

Sophie Hambleton (sophie.hambleton@newcastle.ac.uk), *Institute of Cellular Medicine, Newcastle University, Newcastle upon Tyne NE2 4HH, United Kingdom*

and

Holm H. Uhlig (holm.uhlig@ndm.ox.ac.uk), *Translational Gastroenterology Unit, Experimental Medicine, University of Oxford, John Radcliffe Hospital Oxford, OX3 9DU, United Kingdom*

Phosphoinositide 3-kinase δ (PI3Kδ), a lipid kinase consisting of a catalytic (p110δ, encoded by *PIK3CD*) and a regulatory subunit (p85, encoded by *PIK3R1*), generates the second messenger phosphatidylinositol (3,4,5)-trisphosphate (PIP_3) in the plasma membrane of leukocytes downstream of antigen and cytokine receptors.[1] Signaling via PDK1, AKT, mTOR and downstream targets such as FOXO1, contributes to the metabolic and transcriptional changes required for the expansion, differentiation and effector function of lymphocytes.[1] Activating germline mutations in *PIK3CD* cause the immune dysregulatory disease activated PI3Kδ syndrome (APDS), usually presenting with recurrent sinopulmonary infections in childhood, herpesvirus infections and $CD4^+$ lymphopenia, underscoring the important role of balanced p110δ activity in human adaptive immunity.[1,2] Ablation of p110δ in mice leads to aberrant T cell responses and intestinal inflammation.[3,4] In humans, immune dysregulation including severe colitis is present in many cancer patients who are treated with the p110δ-specific inhibitor Idelalisib.[5] Recently, one patient with autosomal recessive deficiency of p85α[6] and two patients with loss-of function mutations in p110δ[7] have been described who developed humoral immunodeficiency and colitis.

We report a child of consanguineous parentage (fig.1A) who presented at 9 years with bruising and upper gastrointestinal bleeding in association with profound immune-mediated thrombocytopenia. His thrombocytopenia was refractory to corticosteroids, high dose immunoglobulin and splenectomy, culminating in an intracranial bleed requiring surgical evacuation. Immunosuppression was then intensified with cyclosporine, azathioprine and a course of the B-cell-depleting agent Rituximab, with eventual platelet recovery. However, over the next few months he developed first a severe pneumonia followed by intractable diarrhea and striking (~30%) weight loss. Endoscopy revealed enterocolitis, which histologically showed marked apoptosis of crypt epithelial cells, eosinophil and neutrophil infiltration, crypt distortion and crypt abscess formation, with increased CD3+ cells but a paucity of B cells and plasma cells in the lamina propria (fig.1B-C). Viral inclusion bodies were visible, indicating active CMV replication in the gut, accompanied by CMV viraemia ($1.8x10^4$ copies/mL); norovirus genogroup 2 RNA was also detected in stool. Flow cytometric examination of peripheral blood revealed largely normal T cell numbers, modestly reduced naïve T cells, unexceptional T cell mitogenic responses and detectable FOXP3-positive regulatory T cells (supplementary table 1 and supplementary fig.1). Peripheral blood was enriched for effector/memory $CD8^+$ T cells, which expressed high levels of the transcription factor TBET and perforin (fig.1D-E). B cell numbers were low with no class-switched memory B cells and subnormal immunoglobulin levels (IgG 2.5g/L and IgM 0.25g/L), consistent with prior Rituximab therapy and/or a primary B cell abnormality (supplementary table 1).

The patient was treated with total parenteral nutrition and an empiric combination of anti-inflammatory (mesalazine) and antiviral (ganciclovir, foscarnet) therapy, but continued with torren-

tial diarrhoea (3L/day) until the addition of immunosuppression (corticosteroid, cyclosporine, infliximab). Clinical improvement was accompanied by amelioration of inflammatory changes on repeat endoscopic examination. However, weaning of immunosuppressive treatment led to relapse of his gut disease, indicating chronic immune-mediated inflammation.

Haematopoietic stem cell transplantation (HSCT) was therefore performed as a potentially curative procedure. After reduced intensity conditioning (fludarabine 150 mg/m^2, melphalan 140mg/m^2, alemtuzumab 0.6mg/kg), the patient received bone marrow containing 6.9x10^6 $CD34^+$ cells/kg from an 11/12-matched CMV+ve unrelated donor. Cotrimoxazole, foscarnet, liposomal amphotericin, and intravenous immunoglobulin were administered as anti-infective prophylaxis with a combination of cyclosporine and mycophenolate mofetil to prevent graft versus host disease. Unfortunately we observed transplant rejection with early autologous lymphoid reconstitution. We therefore proceeded to a second transplant, using a more myeloablative conditioning regimen (treosulfan 42mg/m^2, fludarabine 150mg/m^2, alemtuzumab 1mg/kg) and peripheral blood stem cells ($CD34^+$ dose 5.3x10^6/kg) from an alternative partially mismatched (11/12) unrelated donor. On this occasion he achieved 100% donor chimerism including lymphoid reconstitution and sustained remission of enterocolitis. Both transplants were complicated by low level CMV viraemia (<2000 copies/ml) and chronic norovirus genogroup 2 in stool. Despite the latter and prior history of prolonged gut failure, the patient required only 9 days' parenteral nutrition in the wake of his first transplant and was otherwise managed with nasogastric feeding and later diet. His 2nd transplant was also complicated by HSV (fever, viraemia, herpetic skin lesion – managed with high dose IV acyclovir) and an asymptomatic pericardial effusion as well as mild pancreatitis (max amylase 600 U/L) which resolved with conservative management. Six months after transplant, the patient returned to the Middle East in a stable condition without signs of enterocolitis or infection and was lost to follow-up.

Suspecting a monogenic immune disorder, we later carried out whole exome sequencing of patient genomic DNA and found the private homozygous frameshift variant c.703_723delinsGT in *PIK3CD*, confirmed by Sanger sequencing (fig.1F). The 21bp deletion coupled to a two bp insertion in exon 5 introduces a premature stop codon (p.Q170Vfs*41) (fig.1G). Rare (<0.001 allele frequency) variants of unknown significance in other immune-related genes were excluded on the basis of poor fit to previously reported phenotypes (*TCIRG1*, *KDM6A, PLCG2*) or autosomal recessive inheritance (*ACP5*, *STK4*), respectively (supplementary table 2).

In accordance with the expected role of PI3Kδ and absence of full-length protein expression (fig. 2A), patient-derived T lymphoblasts were profoundly impaired in their ability to generate PIP_3 upon TCR engagement (fig.2B). TCR- and IL-2-induced phosphorylation of AKT was also reduced in

$CD4^+$ and $CD8^+$ T lymphoblasts, as was IL-2-induced phosphorylation of the mTOR target S6 (fig.2A and supplementary fig.2). Glycolysis stress test showed impaired IL-2-stimulated glycolysis and glycolytic reserve in patient cells, similar to the behaviour of $CD4^+$ and $CD8^+$ T cells treated with Idelalisib (fig.2C-D). These findings show that germline p110δ deficiency impairs lymphocyte metabolism, which we hypothesised might contribute to immunodysregulation through altered T cell polarization and behaviour.

To investigate the cellular immunophenotype within the patient's inflamed gut, we performed immunohistochemistry on colonic biopsies taken prior to HSCT. Relative to healthy age-matched control tissue, there was a modest expansion of $CD8^+$ T cells in the lamina propria and a decrease in the $CD4^+$ to $CD8^+$ T cell ratio (supplementary fig.3). Additionally, we observed a substantial increase in lymphocytes expressing the transcription factor TBET and perforin within both $CD8^+$ and $CD8^-$ T cell compartments (supplementary fig.4)**.**

Owing to the paucity of patient material we were unable to assess directly the function of specific leukocyte subsets but mouse models of PI3Kδ deficiency imply wide-ranging impairments of T-regulatory function, B cell help and $CD8^+$ T cell memory.[3,4] Similar to our patient, p110δ kinase-dead mice spontaneously develop inflammatory bowel disease with crypt abscesses.[3] In these mice, thymic output of Tregs was normal, but Treg trafficking and suppressive activity including IL-10 secretion were disturbed.[4] p110δ kinase-dead mice make weaker responses to antigen exposure than WT mice, both *in vivo* and *in vitro*[3,8], despite apparently normal proliferation and metabolic reprogramming of $CD8^+$ T cells after stimulation of the TCR and the IL-2 receptor[9,10]. Secretion of IFN-γ by effector/memory $CD8^+$ T cells was however significantly reduced by inhibitors of p110δ[11] and AKT[9], consistent with reduced production of IFN-γ in patient cells and potentially relevant to viral susceptibility. This primary immunodeficiency thus highlights the central importance of regulated PI3Kδ activity for immune homeostasis and protective immunity in humans as in mice.

Germline autosomal recessive deficiency of *PIK3CD* has recently been reported in a total of 3 kindreds (supplementary table 3), though two siblings had a second concurrent immune disorder, complicating interpretation of their phenotype[7,12,13]. Of the remaining four patients, all presented with hypogammaglobulinemia and recurrent sinopulmonary infections, some including severe and opportunistic pneumonias. Immune dysregulatory phenomena were also frequent, including inflammatory bowel disease, autoimmune hepatitis and juvenile idiopathic arthritis. Their management involved immunoglobulin replacement and antimicrobial therapy for acute infections, together with anti-inflammatory (mesalazine) or immunosuppressive (steroids and 6-mercaptopurine) therapy where indicated for autoimmune complications.[7,12,13] Although B and NK cell numbers were very low in some patients, others had normal counts and standard laboratory measures of T cell number and function were generally unremarkable. Therefore a high index of

suspicion for an underlying monogenic cause is required in this setting.

In summary, we report a child with homozygous germline loss-of-function mutation in *PIK3CD*, who developed refractory immune thrombocytopenia, inflammatory bowel disease and susceptibility to infection, cured by HSCT. The immune defect was characterized by defective PI3Kδ signaling, altered T cell metabolism and a prominent infiltrate of cytotoxic lymphocytes in the gut lamina propria. Our experience emphasises the potentially life-threatening nature of immune dysregulation in this condition, albeit we were able to gain short-term control with a cocktail of antiviral and immunosuppressive drugs. By analogy with related conditions such as CTLA4 deficiency and STAT3 gain-of-function, HSCT remains an attractive option in severe immune dysregulation of monogenic origin. In the case of therapy with p110δ-specific small molecule inhibitors, we can conclude that autoimmune phenomena such as colitis arise from the same on-target activity that delivers therapeutic benefit by breaking tolerance to malignancy.

Acknowledgments

We thank the patient's family, volunteers and blood donors for participation in this study. This work was supported by the MRC/ESPRC Newcastle Molecular Pathology Node, with technical assistance from Anna Long and Claire Jones. We acknowledge the contributions of the National Institute for Health Research (NIHR) Newcastle Biomedical Research Centre (BRC) and the BRC Gastrointestinal biobank (16/YH/0247), which is supported by the NIHR Oxford Biomedical Research Centre. HHU is additionally supported by the Leona M. and Harry B. Helmsley Charitable Trust, and the Crohn's & Colitis Foundation of America. SH is supported by the Sir Jules Thorn Trust, Bubble Foundation and the Wellcome Trust (WT). CAL is supported by the NIHR. KO is funded by the MRC, WT, BBSRC and GSK. ACh is supported by WT and GSK. The views expressed are those of the authors and not necessarily those of the NHS, the NIHR or the Department of Health.

Conflicts of interest

HHU received research support or consultancy fees from UCB Pharma, Eli Lilly, Boehringer Ingelheim, Pfizer, Celgene and AbbVie. SH received consultancy fees from UCB Pharma and a speaking honorarium from Biotest. KO and ACh report research grants from GSK (funding KC); KO reports personal fees from Karus (scientific advisory board), and speaker fees from Gilead, during the conduct of the study. DA reports grants from Eli Lilly and Company, and from UCB Pharma, during the conduct of the study. CAL received research support from Genentech and Roche. Other authors have no conflict of interest to report.

References:

1. Lucas CL, Chandra A, Nejentsev S, Condliffe AM, Okkenhaug K. PI3Kδ and primary immunodeficiencies. Nat Rev Immunol. 2016;16(11):702–714.

2. Coulter TI, Chandra A, Bacon CM, et al. Clinical spectrum and features of activated phosphoinositide 3-kinase δ syndrome: A large patient cohort study. J Allergy Clin Immunol. 2017;139(2):597-606.

3. Okkenhaug K, Bilancio A, Farjot G, et al. Impaired B and T cell antigen receptor signalling in p110δ PI 3-kinase mutant mice. Science. 2002;297(5583):1031–1034.

4. Patton DT, Garden OA, Pearce WP, et al. Cutting Edge: The Phosphoinositide 3-Kinase p110 Is Critical for the Function of CD4+CD25+Foxp3+ Regulatory T Cells. J Immunol. 2006;177(10):6598–6602.

5. Stark AK, Sriskantharajah S, Hessel EM, Okkenhaug K. PI3K inhibitors in inflammation, autoimmunity and cancer. Curr Opin Pharmacol. 2015;23:82–91.

6. Conley ME, Dobbs AK, Quintana AM, et al. Agammaglobulinemia and absent B lineage cells in a patient lacking the p85α subunit of PI3K. J Exp Med. 2012;209(3):463–470.

7. Sogkas G, Fedchenko M, Dhingra A, Jablonka A, Schmidt RE, Atschekzei F. Primary immunodeficiency disorder caused by phosphoinositide 3–kinase δ deficiency. J Allergy Clin Immunol. 2018;142(5):1650-1653.

8. Pearce VQ, Bouabe H, MacQueen AR, Carbonaro V, Okkenhaug K. PI3Kδ Regulates the Magnitude of CD8+ T Cell Responses after Challenge with Listeria monocytogenes. J Immunol. 2015;195(7):3206-3217.

9. Macintyre AN, Finlay D, Preston G, et al. Protein kinase B controls transcriptional programs that direct cytotoxic T cell fate but is dispensable for T cell metabolism. Immunity. 2011;34(2):224-236.

10. Finlay DK, Rosenzweig E, Sinclair LV, et al. PDK1 regulation of mTOR and hypoxia-inducible factor 1 integrate metabolism and migration of CD8+ T cells. J Exp Med. 2012;209(13):2441-2453.

11. Soond DR, Bjørgo E, Moltu K, et al. PI3K p110delta regulates T-cell cytokine production during primary and secondary immune responses in mice and humans. Blood. 2010;115(11):2203-2213.

12. Sharfe N, Karanxha A, Dadi H, et al. Dual loss of p110d PI3-kinase and SKAP (KNSTRN)

expression leads to combined immunodeficiency and multisystem syndromic features. J Allergy Clin Immunol. 2018;142(2):618-629.

13. Zhang KJ, Husami A, Marsh R, Jordan MB. Identification of a phosphoinositide-3 kinase (PI-3K) p110d (PIK3CD) deficient individual. J Clin Immunol. 2013;33:673-674.

Figure Legends

Figure 1: *PIK3CD* mutation in a patient with immunodeficiency and immune dysregulation.

(**A**) Pedigree.

(**B**) Haematoxylin & eosin staining showing colitis and crypt abscess formation.

(**C**) Immunostaining for CD3 (gold) and CD20 (purple); P1, patient; HD, healthy donor.

(**D**) CCR7 and CD45RA staining and quantification of memory CD8+ cells among CD25-CD8+ cells.

(**E**) Expression of perforin and transcription factor TBET in naïve and memory CD8+ T cells.

(**F**) Sanger sequencing confirming frameshift deletion plus 2bp insertion.

(**G**) p110δ schematic showing p.Q170Vfs*41 and previously reported mutations.

Figure 2: Functional impact of *PIK3CD* mutation.

(A) Immunoblotting of p110δ, AKT, $pAKT^{T308}$, $pERK^{T202/Y204}$, $pS6^{S235/236}$ and beta-actin in control (HD) and patient (P1) CD4+ and CD8+ T lymphoblasts with and without CD3 stimulation.

(B) PIP_3 quantification before/after TCR stimulation.

(C) and (**D)** Extracellular acidification rate (Seahorse assay) and quantification of glycolysis in IL-2-stimulated T lymphoblasts of HD and P1 (**C**) or HD cells treated with Idelalisib (**D**). Three independent experiments with 5-8 technical replicates each; values are plotted as mean of three time points for each injection and each replicate (**p<0.01 and ***p<0.001, Mann-Whitney U test).

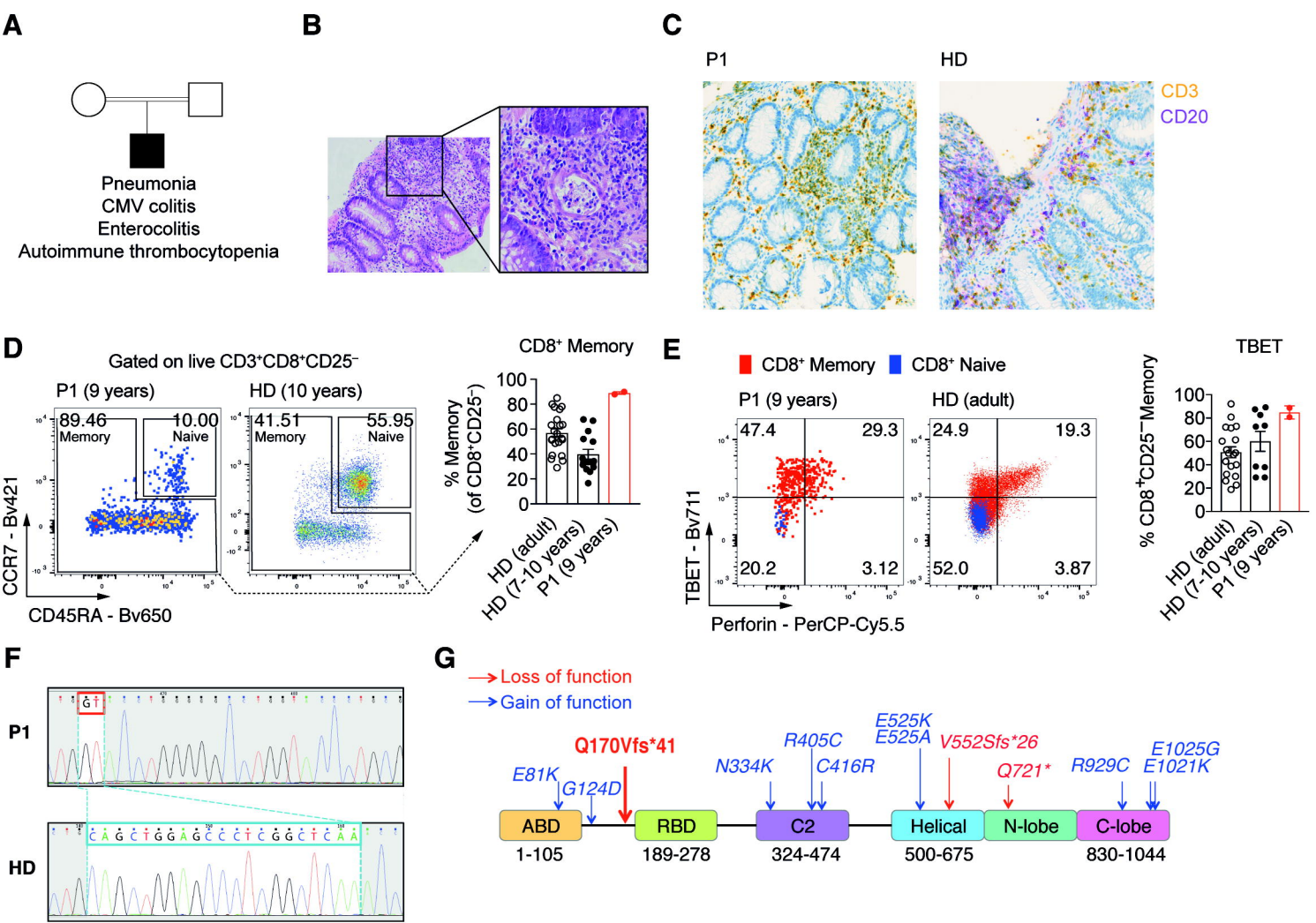
A
Pneumonia
CMV colitis
Enterocolitis
Autoimmune thrombocytopenia
B
C
P1
HD
CD3
CD20
D
Gated on live CD3+CD8+CD25−
P1 (9 years)
HD (10 years)
89.46
Memory
10.00
Naive
41.51
Memory
55.95
Naive
CCR7 - Bv421
CD45RA - Bv650
CD8+ Memory
% Memory (of CD8+CD25−)
HD (adult)
HD (7-10 years)
P1 (9 years)
E
CD8+ Memory
CD8+ Naive
P1 (9 years)
HD (adult)
47.4
29.3
20.2
3.12
24.9
19.3
52.0
3.87
TBET - Bv711
Perforin - PerCP-Cy5.5
TBET
% CD8+CD25− Memory
HD (adult)
HD (7-10 years)
P1 (9 years)
F
P1
HD
G
Loss of function
Gain of function
Q170Vfs*41
E81K
G124D
N334K
R405C
C416R
E525K
E525A
V552Sfs*26
Q721*
R929C
E1025G
E1021K
ABD
1-105
RBD
189-278
C2
324-474
Helical
500-675
N-lobe
C-lobe
830-1044

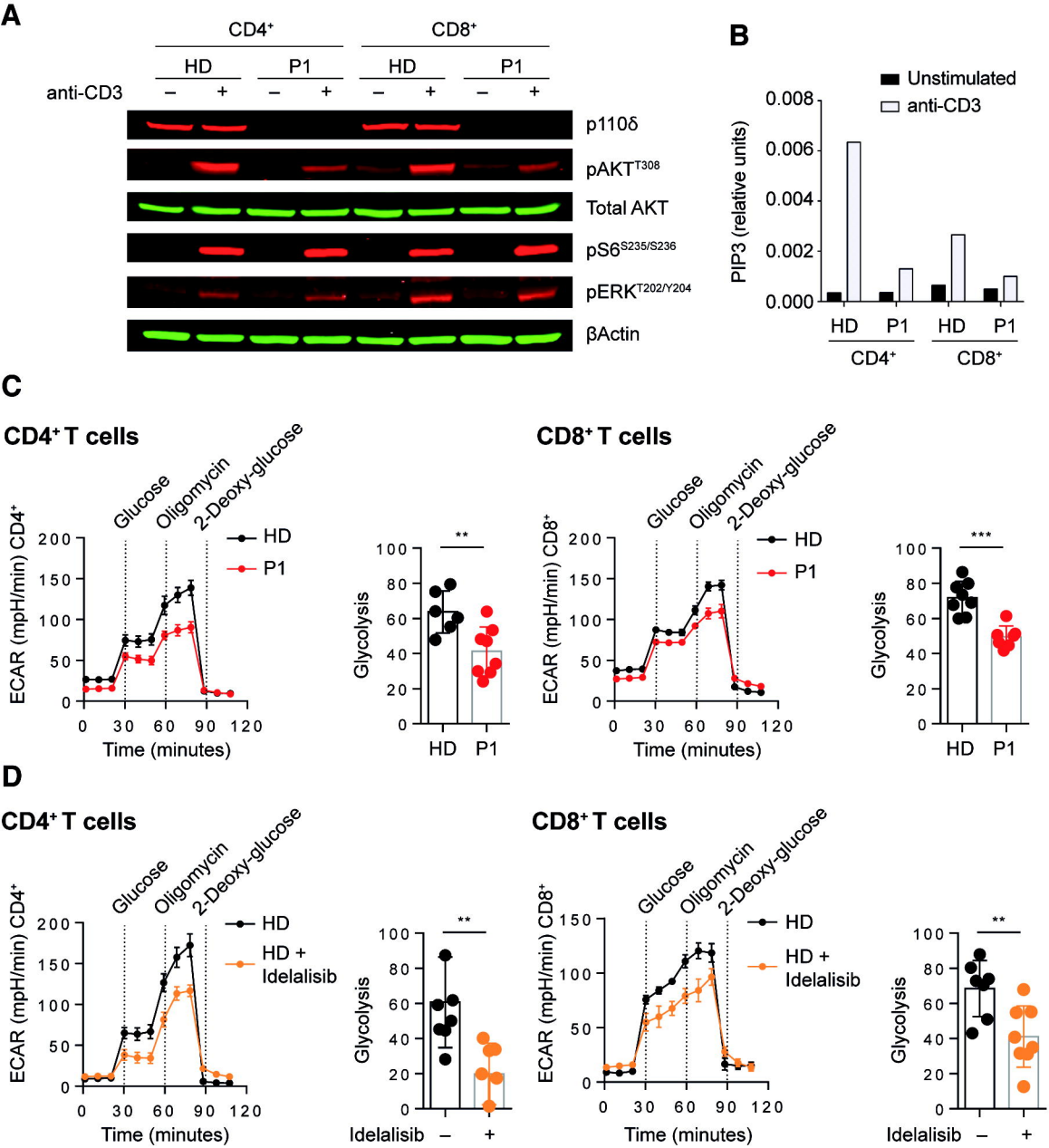
A
CD4+
CD8+
HD
P1
HD
P1
anti-CD3
– + – + – + – +
p110δ
pAKT T308
Total AKT
pS6 S235/S236
pERK T202/Y204
βActin
B
Unstimulated
anti-CD3
PIP3 (relative units)
0.008
0.006
0.004
0.002
0.000
HD P1 HD P1
CD4+ CD8+
C
CD4+ T cells
Glucose
Oligomycin
2-Deoxy-glucose
ECAR (mpH/min) CD4+
HD
P1
Time (minutes)
Glycolysis
**
HD P1
CD8+ T cells
ECAR (mpH/min) CD8+
***
D
CD4+ T cells
HD + Idelalisib
Idelalisib – +
CD8+ T cells

SUPPLEMENTARY INFORMATION

Methods

Patient

Patient and controls were recruited with written informed consent of the individuals and/or their parents to participate in research, approved by the National Research Ethics Service. Patients were recruited via the Great North Biobank (10/H0906/22) and healthy donors were recruited via the Oxford Gastrointestinal Illness biobank (16/YH/0247).

Whole exome sequencing

Whole exome capture from patient whole blood DNA was achieved using the Agilent SureSelect V5 kit and libraries subsequently prepared for paired-end sequencing. Libraries were sequenced on an Illumina NextSeq instrument by a commercial sequencing provider (Oxford Gene Technology, UK). Read quality was assessed using the FastQC and MultiQC tools.[1,2] Reads were aligned to the hg19 assembly of the human reference genome, and analysed according to Genome Analysis Toolkit (GATK) best practices[3], as follows: the raw alignment was realigned around indels, quality scores recalibrated (BQSR), and duplicates marked using the Picard suite. Genotyping was performed using a combination of the HaplotypeCaller from GATK in gVCF mode, and JointCalling program leveraging an in-house exome catalogue. To avoid false positive calls, variant quality score recalibration (VQSR) was performed on the raw variant callsets for indels and SNPs. Downstream analysis was carried out using the web-based analytics application Ingenuity Variant Analysis (Qiagen) with the following selection criteria: call quality ≥20, read depth ≥10, allele fraction ≥45%; allele frequency ≤0.01% (ExAc); frameshift, in-frame indel, stop codon change, deleterious missense (by SIFT/Polyphen), or splice site disruption. The candidate *PIK3CD* variant was validated by Sanger sequencing (SourceBioscience) in patient genomic DNA, following PCR amplification using primers designed with Primer3web version 4.1.0 (forward primer: GGCCTCCACGAGTTTGACT, reverse primer: GCGGATGACTGAGGAGTTTC).

PBMC isolation, generation of T cell lines and T cell maintenance

PBMCs were isolated by means of density centrifugation over Ficoll-Paque and resuspended in complete RPMI media. For T cell expansion, either of the following 2 methods was used: 1) Cells were cultured for 72 hrs in the presence of anti-CD3 (1ug/ml), anti-CD28 (1ug/ml) and IL-2 (20 ng/ml). Once the T cells were differentiated to T cell blasts, a further expansion was done in the presence of IL-2 for another 72-96 hrs. 2) T cells were expanded from $0.3x10^6$ total PBMCs by stimulation with phytohaemagglutinin (PHA, 1 µg/mL; Remel) in the presence of $2.5x10^4$ irradiated allogeneic (45 Gy) PBMCs and cultured for 21 days in IL-2 containing medium (500 U/mL) as previously described.[4] For the generation of T cell lines, cells were FACS-sorted to >98% purity based

on the surface expression of $CD3^+CD4^+CD8^-$ and $CD3^+CD8^+CD4^-$ marker combinations (antibodies used, and surface staining methodology as described in the section "analysis of surface marker expression"). T cells were expanded by culturing $5x10^5$ cells in the presence of $2.5x10^4$ irradiated (45 Gy) allogeneic PBMCs/50 μl culture for 21 days in medium supplemented with IL-2 (500 U/mL). Cell sorting was performed using a FACSAria III (BD Biosciences).

T cell lines were cultured thereafter in complete RPMI with L-glutamine (Sigma) supplemented with 5 % (v/v) human serum (NHS Blood Center Oxford), non-essential amino acids (Gibco); 1 mM sodium pyruvate (Gibco) and 100 U/mL penicillin and 10 μg/mL streptomycin (Sigma), hereafter called complete medium. Where indicated 500 U/mL IL-2 was added to the culture medium (produced in house from IL-2T6 culture supernatants).

PIP_3 quantification

PIP_3 was quantified as described[5]. T cells were isolated from PBMCs using immunomagnetic negative selection kit (Stemcell T cell isolation kit). The purified T cells were stimulated with anti-CD3 (1μg/ml) and anti-CD28 (2μg/ml) antibodies followed by crosslinking with goat anti-mouse IgG (1:500) antibodies for 1 min at 37˚C. After stimulation of T cells, reactions were terminated by addition of 750 µl kill solution and samples were immediately frozen. Samples were kept in a freezer at -80°C until they were processed. Samples were thawed and 10 µl of C16/C17 PIP_2 and PIP_3 internal standard (ISD) was added. After 5 min at room temperature, 725 µl $CHCl_3$ and 170 µl 2M HCl were added to the samples. After that, samples were centrifuged and the lower organic phase was collected. 708 µL of pre-derivatisation wash (upper phase) was added, vortexed and samples were centrifuged again. The lower phase was then collected in a fresh tube for derivatisation. 50 µl 2M TMS-diazomethane was added to the lipid extracts and they were incubated for 10 min at room temperature. The reaction was stopped by addition of 6 µl of glacial acetic acid and the samples were washed twice with 700 µl post-derivatisation buffer (upper phase). After the final wash, 100 µl of MeOH:H_2O (9:1) were added to the samples and they were dried under a stream of nitrogen at room temperature. Samples were then re-dissolved in 80 µl of MeOH, sonicated and 20 µl of water was added. The samples were then sent for a mass spectrometry analysis Samples were analysed on a ABSciex QTRAP 4000 connected to a Waters Acquity UPLC system. Integrated area of PIP_3 was corrected for recovery against the PIP_3 internal standard and then normalized to the integrated area of PIP_2 corrected for recovery against the PIP_2 internal standard. The Mass spec data are expressed as ratio of the quantity of the intracellular PIP_3 divided by that of the PIP_3 internal standard and normalized according to the intracellular PIP_2 divided by that of the PIP_2 internal standard.

Analysis of T cell receptor and IL-2 receptor signaling by immunoblotting

T cell lines were extensively washed before serum starvation for 4h in RPMI medium without supplements. Cells were resuspended at 5 $x10^6$ cells/mL and aliquoted as 100µl per test tube. Cells were then cooled on ice for 15 min. For cell activation via the TCR, cells were incubated with 1µg/mL

OKT3 (Biolegend) and 2µg/mL anti-CD28 on ice for 5 min followed by addition of 5µg/mL goat anti-mouse crosslinking antibody (Biolegend) and a further 5 min incubation on ice. Stimulation was achieved by placing the cells into a 37°C water bath for 5 min. For unstimulated cells, the antibodies were added but the cells were not warmed to 37°C. For cell activation via the IL-2 receptor, cells were stimulated with 100ng/mL rhIL-2 (Peprotech) for the indicated times. Cells were then lysed in ice-cold lysis buffer, and lysates were separated by electrophoresis, transferred to a PVDF membrane (Immobilon-P, Millipore) and probed for various signaling components by western blot, using the following antibodies (from Cell Signaling Technology, unless otherwise indicated): anti-p110δ (H-219) (Santa Cruz Biotechnology; clone Sc7176), anti-phospho-STAT5 (Tyr694) (D47E7) Rabbit mAb (# 4322), anti-phospho-AKT (Thr308) (244F9) Rabbit mAb (# 4056), anti-AKT (11E7) Rabbit mAb (# 4685) or anti-AKT (2H10) Mouse mAB (# 2967), anti-phospho-S6 (S235/S236) (D57.2.2E) Rabbit mAB (# 4858), anti-phospho-ERK p44/42 MAPK (T202/Y204) Rabbit Ab (# 9101), and anti-rabbit IgG or anti-mouse IgG HRP-linked secondary antibodies (# 7074, #x). Anti-histone H3 (clone D1H2; # 4499) and anti-βActin (C4; Santa Cruz Biotechnology, clone Sc-47778) antibodies were used as loading control.

Analysis of AKT and S6 phosphorylation by flow cytometry

T cell lines were starved of IL-2 for 12 hours followed by extensive washing in RPMI supplemented with 25mM HEPES (Sigma; Cat.# H0887) and 0.5% human serum. Stimulation was performed in complete RPMI by addition of IL-2 (100 U/ml). Following indicated incubation times cells were fixed at 37°C for 15 minutes in 3.7% Formaldehyde (Sigma; Cat.# F8775). Cells were then permeabilised in -20°C 90% Methanol (Merck; Cat.# 106035) on ice. Staining for phosphorylated AKT and S6 was performed at RT for 60 minutes in PBS supplemented with 0.5% Bovine serum albumin (BSA; Sigma; Cat.# A9418). Following antibodies were used for analysis: anti-pAKT(S437) (Cell signalling; clone: M-89-61), and anti-pS6(pS235/p236) (BD Biosciences; clone: N7-548).

Ex vivo analysis of surface marker expression

The expression of surface markers was analysed by incubating cells with the relevant antibody conjugates for 15 min at room temperature in PBS supplemented with 0.5% (v/v) human serum. For the exclusion of dead cells during the analysis, cells were stained prior to fixation using Fixable Viability Dye eFluor® 780 (eBioscience) according to the manufacturer's instructions. The following fluorophore-conjugated antibodies were used for analysis: anti-CD3 (BD Biosciences; clone UCHT1), anti-CD4 (Biolegend; clone RPA-T4), anti-CD8 (Biolegend; clone SK1), anti-CD14 (Biolegend; clone M5E2), anti-CD19 (BD Biosciences; clone SJ25C1), anti-CD25 (Biolegend; clone MA-A251), anti-CD45RA (Biolegend; clone HI100), anti-CD56 (BD Biosciences; clone NCAM16.2), anti-CD127 (Biolegend; clone A019D5); anti-CCR7 (Biolegend; clone G043H7).

Analysis of transcription factor and perforin expression in PBMC

For the analysis of transcription factor and perforin expression, PBMCs were stained for surface markers as indicated above followed by fixation and permeabilisation using the Transcription Factor Staining Buffer Set (eBioscience) according to the manufacturer's instructions. For the exclusion of dead cells during the analysis, cells were stained prior to fixation using Fixable Viability Dye eFluor® 780. The following fluorophore-conjugated antibodies were used: anti-TBET (Biolegend; clone 4B10), anti-FOXP3 (eBioscience; clone: PCH101), anti-Perforin (Biolegend; clone B-D48).
Samples were acquired on a BD Fortessa or BD LSRII and data were analysed using FlowJo software (Tree Star). Gating was performed using isotype or unstimulated controls.

Metabolic analysis

Glycolysis stress test XFe96 (Agilent technologies) was performed as per manufacturer's protocol. CD4+ and CD8+ T cell lines were starved of IL-2 for 12 hours in complete medium followed by extensive washing in complete medium. Cells were plated at a density of 250,000 cells per well in Seahorse base media containing 1% FCS, 2μM glutamine, 1μM sodium pyruvate and 50U/ml of IL-2 (R&D Systems). The plate was then incubated in a CO_2-free incubator for one hour. Extracellular acidification rate (ECAR) was recorded at baseline, after glucose, oligomycin and 2-Deoxy-Glucose injection respectively. The assay was performed in technical replicates of 8 and repeated 3 independent times. Glycolysis, glycolytic capacity and glycolytic reserve were calculated as per manufacturer's instructions. Idelalisib (CAL101) treatment was or was not carried out for 48hr on healthy donor CD4+ and CD8+ T cell lines before performing the Seahorse assay as described above.

Immunohistochemistry

Immunohistochemical analysis was performed on formalin-fixed and paraffin-embedded (FFPE) colonic biopsies obtained by colonoscopy. 4μm sections were stained using a Discovery Ultra autostainer (Ventana Medical Systems, Tucson, AZ) using HRP-activated, or alkaline phosphatase chromogenic detection kits. The following primary antibodies were used: anti-CD3; Mouse clone LN10, Leica; anti-CD20, clone L26, Dako; anti-CD4, Rabbit SP35, Ventana; anti-CD8, clone SP57, Ventana; anti-Perforin, clone 5810, Abcam; and anti-Tbet, clone MRQ-46, Ventana. Sections were counterstained with haematoxylin. Multispectral scanning of stained slides at 10x magnification was undertaken using a Vectra 3.0 Automated Quantitative Pathology Imaging System (PerkinElmer, Hopkinton, MA). InForm Cell Analysis software (v2.0, PerkinElmer) allowed image deconvolution. Tissue segmentation algorithms were developed for automated delineation of intestinal epithelium and lamina propria, which was then applied to all cases, and the accuracy of segmentation was optimised by manual correction. Individual cells in both tissue compartments were identified using a cell segmentation algorithm, based upon the identification of cell nuclei. A binary approach (positive/negative) was used to score the relative expression of each; visual cues were used to distinguish positive staining compared to background, and thresholds were assigned. These data were exported and compiled in MATLAB (v2016b MathWorks, Natick, MA).

Statistics

Differences were analysed using Mann Whitney U test or ANOVA using GraphPad Prism v7 (GraphPad Software).

Supplementary References:

1. Andrews S. FastQC: a quality control tool for high throughput sequence data. 2010. Available online at: http://www.bioinformatics.babraham.ac.uk/projects/fastqc
2. Ewels P, Magnusson M, Lundin S, Käller M. MultiQC: summarize analysis results for multiple tools and samples in a single report. Bioinformatics. 2016;32(19):3047-8.
3. Van der Auwera GA, Carneiro MO, Hartl C, et al. From FastQ data to high confidence variant calls: the Genome Analysis Toolkit best practices pipeline. Curr Protoc Bioinformatics. 2013;43:11.10.1-33.
4. Geiger R, Duhen T, Lanzavecchia A, Sallusto F. Human naive and memory CD4 $^{+}$ T cell repertoires specific for naturally processed antigens analyzed using libraries of amplified T cells. J Exp Med. 2009;206(7):1525–34.
5. Clark J, Anderson KE, Juvin V, et al. Quantification of PtdInsP3 molecular species in cells and tissues by mass spectrometry. Nat Methods. 2011;8(3):267-72.

Supplementary Figures:

Supplementary Fig 1

Normal frequency of FOXP3 expression in patient CD4+ T cells.

Intracellular staining for FOXP3 in patient (P1) and control (HD) peripheral blood CD4+ T cells. HD (adult): n=24, HD (7-10 years): n=5, P1 (9 years): n=1 (two independent replicates).

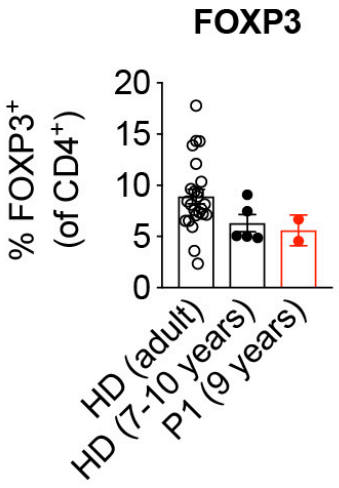

Supplementary Fig 2

Defective IL-2 signaling to AKT in p110δ-deficient CD4+ and CD8+ T cell lines.

(A) Immunoblot showing timecourse of phosphorylation response to IL-2 in CD4+ T lymphoblasts from patient (P1) and control (HD). (**B)** Timecourse analysis and histogram examples (pAKT: 15 minutes stimulation; pS6: 30 minutes stimulation) of AKT phosphorylation and (**C**) S6 phosphorylation response to IL-2 in CD4+ and CD8+ T lymphoblasts from patient (P1) and control (HD) by flow cytometry. Non-stimulated (ctrl) cells were used as control and results presented as relative mean fluorescence intensity (rMFI). Results from two independent experiments and each two technical replicates are shown (HD: n= 2; P1: n=1). *p<0.05, **p<0.01. False discovery rate-corrected two-way ANOVA.

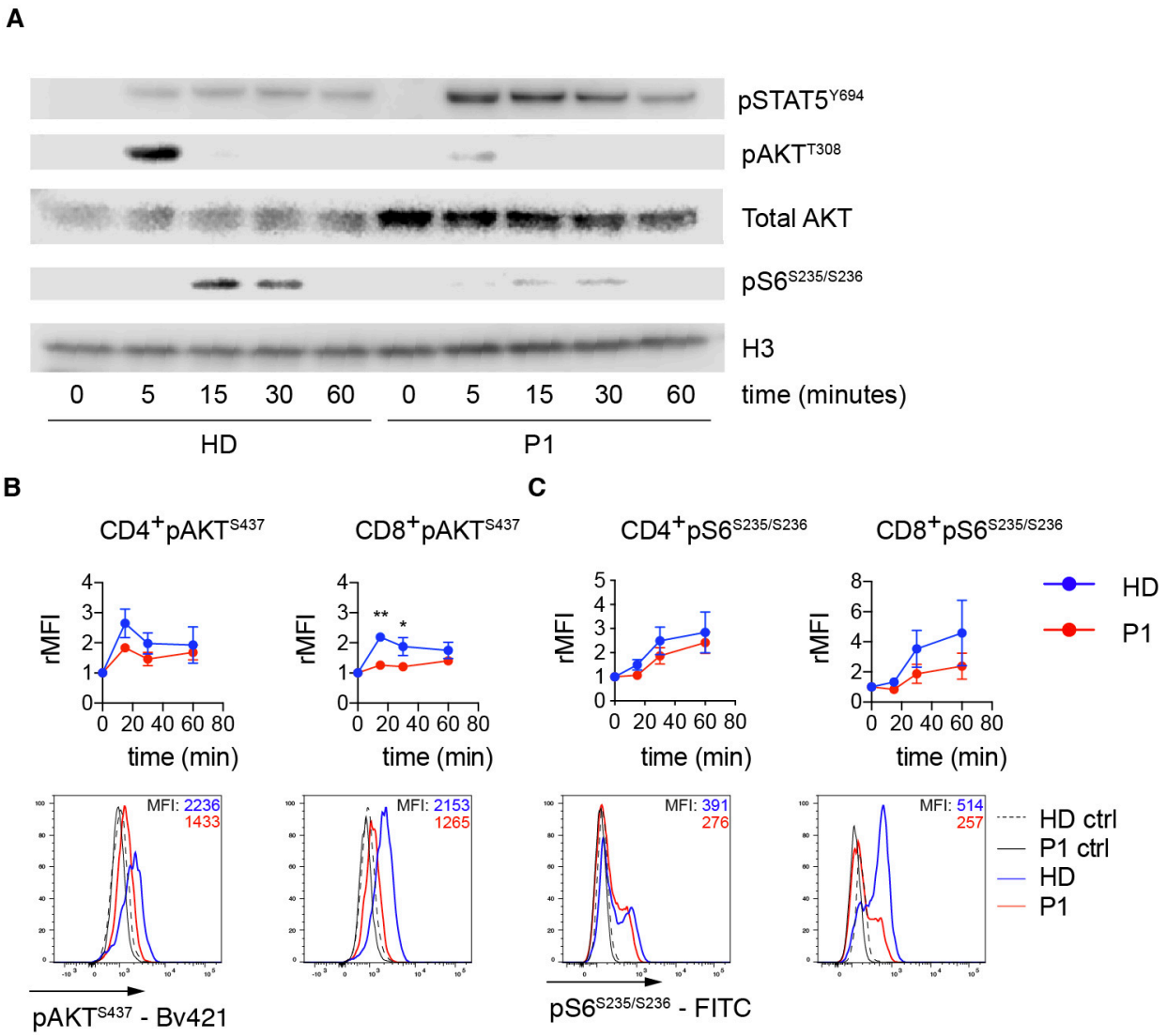

Supplementary Fig 3

CD8 intestinal T cell expansion in a patient with p110δ-deficiency.

Representative immunostaining and quantification of CD4+ (gold) and CD8+ (purple) cells in patient (P1) and control (HD) colonic biopsy tissue sections.

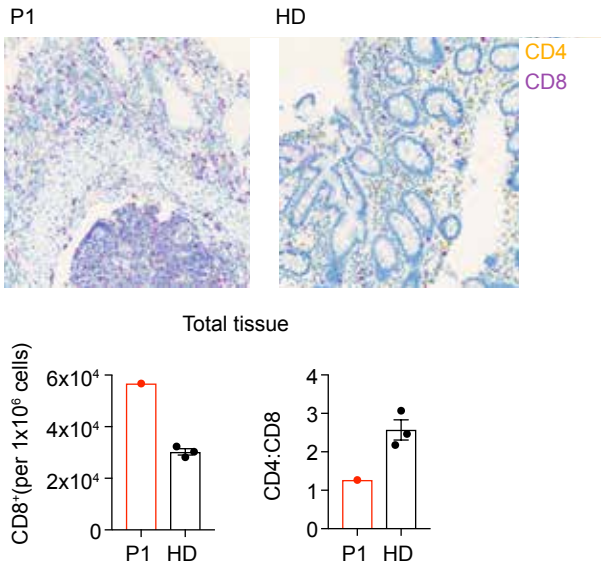

Supplementary Fig 4

Increased intestinal TBET and perforin staining in a patient with p110δ-deficiency.

Immunostaining for TBET (gold; left hand panels) and perforin (purple; right hand panels) in patient (P1) and control (HD) colonic biopsy tissue sections. Quantification of the respective cells is shown below.

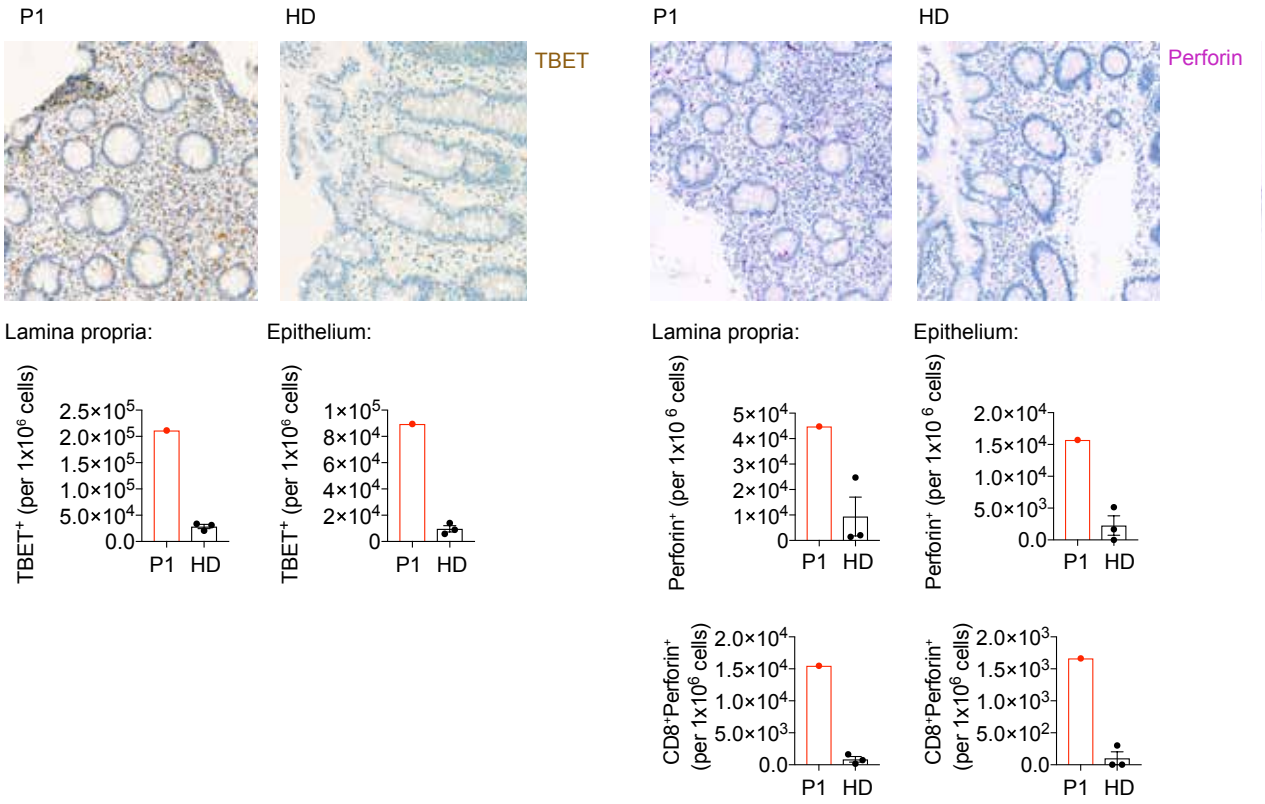

Supplementary Table 1:

Immune parameters in patient 1 with *PIK3CD* p.Q170Vfs*41 variant.

Parameter	Patient values**	Normal range (units)§
T cells	3794 - 5463	1400-2300
CD4+ T cells	1940 - 2398	900-5500
CD8+ T cells	1680 - 2866	400-2300
Naïve CD4+ (CD45RA+CD27+)	324	
Naïve CD8+ (CD45RA+CD27+)	162	
Double negative T (CD4-CD8-)	<1	<1(%)
FOXP3+ (% of CD4+) T cells	5.6	6.3 (%)#
TCRαβ (of T cells)	91-93	(%)
TCRVβ usage	polyclonal	
HLA-DR+ T cell	13	(%)
B cells	70	600-3100
CD27+IgD- B	absent	
NK cells	282 - 471	100-1400
IgG	2.5*	3.7-15.0 (g/L)
IgA	0.43 - 0.68	0.3-1.2 (g/L)
IgM	0.25 - 0.4	0.5-2.2 (g/L)
IgE	18	0-60 (IU/mL)

** Results obtained prior to commencement of immunosuppressive therapy

§ Units = cells/μl unless otherwise stated.

* Subsequently maintained on immunoglobulin replacement

Age matched healthy donors (7-10 years old)

Supplementary Table 2. Rare WES findings in IUIS-designated PID genes*.

Gene	Variant	Genotype	ExAc	Impact predictions	Gene name	Associated diseases (OMIM)
PIK3CD	frameshift	hom.	0	CADD 29.0	Phosphatidyl-inositol-4,5-Bis-phosphate 3-Kinase catalytic Subunit Delta	Immunodeficiency 14, AD (APDS) Immune dysregulation & immunodeficiency, AR [current study]
TCIRG1	c.170C>T p.Ala57Val	T/T	0.00029	CADD 13.43 Mutation taster: disease causing	T Cell Immune Regulator 1, ATPase H+ Transporting V0 Subunit A3	Osteopetrosis, AR
KDM6A	c.2732G>C p.Ser911Thr	C	0.000069	CADD 18.43 Mutation taster: disease causing	Lysine Demethylase 6A	Kabuki syndrome, X-linked
PLCG2	c.3075C>G p.His1025Gln	C/G	0.000017	CADD 9.677 Mutation taster: disease causing PolyPhen: benign	Phospholipase C Gamma 2	Autoinflammation, antibody deficiency, and immune dysregulation syndrome, AD; Familial cold autoinflammatory syndrome 3, AD
ACP5	c.839G>A p.Arg280His	C/T	0.000008	CADD 28.1 Mutation taster: disease causing PolyPhen: benign	Acid Phosphatase 5, Tartrate Resistant	Spondyloenchondrodysplasia with immune dysregulation, AR
STK4	c.872G>A p.Arg291Gln	G/A	0.000017	CADD 23.0 Mutation taster: disease causing PolyPhen: benign	Serine/Threonine Kinase 4	T-cell immunodeficiency, recurrent infections, autoimmunity, and cardiac malformations, AR

*rare: <0.001 allele frequency; IUIS gene: PID disease genes specified by the International Union of Immunological Societies (IUIS) [Picard C, Bobby Gaspar H, Al-Herz W, Bousfiha A, Casanova JL, Chatila T, et al. International Union of Immunological Societies: 2017 Primary Immunodeficiency Diseases Committee Report on Inborn Errors of Immunity. J Clin Immunol. 2018;38:96-128.]

Abbreviations:

WES, Whole exome sequencing

OMIM, Online Mendelian Inheritance in Man

hom., homozygous

CADD, combined annotation dependent depletion

APDS, Activated PI3K Delta Syndrome

AD, autosomal dominant

AR, autosomal recessive

Supplementary Table 3. Comparison of current and previously described patients with AR *PIK3CD* deficiency.

Patient		current	P2	P3	P4	P5	P6
***PIK3CD* gene variant(s)**		hom. c.703_723delinsGT	compound het missense & premature stop	hom c.2161C>T (plus hom variant in *KNSTRN*)		hom c.1653_1653delG	
Effect on protein	variant	p.Q170Vfs*41		p.Q721*		p.V552Sfs*26	
	p110δ expression	absent	reduced	absent		ND	
Immune disease phenotype	age of onset	9y	childhood	5m	<1m	2y	2m
	infections	pneumonia CMV colitis	recurrent RTI, septic arthritis, PCP	recurrent RTI, recurrent UTI, oral thrush	PCP, PIV pneumonia, oral thrush	recurrent RTI, chronic rotavirus gastroenteritis, Klebsiella	recurrent RTI, metacarpal osteomyelitis
	immune dysregulation	ITP IBD	mild IBD, autoimmune hepatitis	arthritis, psoriasis			IBD (Crohn's)
Other clinical features				dysmorphism, feeding difficulties, developmental delay			
Laboratory features	CD3+ T cell number	normal[¶]	moderately low	normal		normal	normal
	T cell proliferation	normal[¶¶]	ND	moderately reduced		normal	ND
	B cell number	reduced (70-228/µl)	near absent	borderline low		near absent (17/µl)	near absent (29/µl)
	NK cell number	normal	present	borderline low		normal	
	NK cell function	ND	reduced	ND		reduced	
	immunoglobulins	low[¶¶¶]	low	low		low	borderline low
Reference		current report	Zhang (2013)[9]	Sharfe et al (2018)[8]		Sogkas et al (2018)[7]	

Abbreviations (Supplementary Table 3):

CMV cytomegalovirus
hom homozygous
IBD inflammatory bowel disease
ITP immune-mediated thrombocytopenic purpura (platelet antibody positive)
ND not done
PCP Pneumocystis jirovecii pneumonia
PIV Parainfluenza virus
RTI respiratory tract infection
UTI urinary tract infection

[¶] normal CD4 and CD8 cell numbers, reduced naïve (CD27+CD45RA+) T cells, normal CD4+CD25hiCD127- T regulatory cells
[¶¶] normal T cell proliferation in response to PHA, CD3 +/- IL-2, PMA & ionomycin